Published in : Journal of Building Performance Simulation (2016)

Status : Postprint (Author's version)

A general methodology for optimal load management with distributed renewable energy generation and storage in residential housing

E. Georges[1]*, J. E. Braun[2], V. Lemort[1]

[(1)] Thermodynamics Laboratory, University of Liège, Liège, Belgium
[(2)] Ray W. Herrick Laboratories, Purdue University, West-Lafayette, Indiana, USA

Abstract

In the U.S., buildings represent around 40% of the primary energy consumption and 74% of the electrical energy consumption (U.S. DOE, 2012). Incentives to promote the installation of on-site renewable energy sources have emerged in different states, including net metering programs. The fast spread of such distributed power generation represents additional challenges for the management of the electricity grid and has led to increased interest in smart control of building loads and demand response programs.

This paper presents a general methodology for assessing opportunities associated with optimal load management in response to evolving utility incentives for residential buildings that employ renewable energy sources and energy storage. An optimal control problem is formulated for manipulating thermostatically controlled domestic loads and energy storage in response to the availability of renewable energy generation and utility net metering incentives. The methodology is demonstrated for a typical American house built in the 1990s and equipped with a single-speed air-to-air heat pump, an electric water heater and PV collectors. The additional potential associated with utilizing electrical batteries is also considered. Load matching performance for on-site renewable energy generation is characterized in terms of percentage of the electricity production consumed on-site and the proportion of the demand covered. For the purpose of assessing potential, simulations were performed assuming perfect predictions of the electrical load profiles. The method also allows determination of the optimal size of PV systems for a given net-metering program.

Results of the case study showed significant benefits associated with control optimization including an increase of load matching between 3 and 28%, with the improvement dependent on the net-metering tariff and available storage capacity. The estimated cost savings for the consumer ranged from 6.4 to 27.5% compared to no optimization with a unitary buy-back ratio, depending on the available storage capacity. Related reduction in CO2 emissions were between 11 and 46%. Optimal load management of the home thermal systems allowed an increase in the optimal size of the PV system in the range of 13 to 21%.

Keywords: net metering, load matching, heat pump, optimal control, linear programming

1. Introduction

Since the late 1990s, many states in the U.S. have started incentive programs to promote the installation of on-site renewable energy sources, such as tax incentives, low-interest loans and net energy metering. On the one hand, the introduction of distributed electricity generation and the fluctuating character of renewable energy sources complicate the planning and operation of the electric utility system and may affect its reliability. At the distribution level, the main negative impacts are the overload of feeders and transformers and the risks of overvoltage and power quality disturbances (Bollen and Hassan, 2011). Such issues are illustrated, for example, in Baetens et al. (2012) for a net zero energy neighborhood with building-integrated photovoltaic (PV) systems. The fraction of local PV supply wasted by

inverter curtailing and peak transformer loads was estimated to be between 14% and 47%. On the other hand, decentralized electricity production helps decrease peak electrical demand, system losses and grid reinforcement needs (Mondol, Yohanis and Norton, 2009). In this context, demand response programs, smart controls of thermostatically-controlled building loads and prosumer storage are seen as key features for improving grid reliability and reducing infrastructure costs (Kamgarpour et al., 2013, and IEA, 2014). Sartori et al. (2012) suggested that buildings can help reduce the burden on the electricity grid through load shifting in response to signals from the grid such as power exchange (Miara et al., 2014), voltage level (De Coninck et al., 2013), time frames or price signals (Halvgaard et al., 2012). In particular, if buildings are equipped with on-site generation (e.g., PV collectors), then load shifting can be used to diminish the impact of distributed energy production by promoting better load matching.

Two mainstream approaches are presented in the literature to investigate the potential benefits of decentralized power units: a centralized approach and a decentralized approach. In the centralized approach, the problem is studied across a portfolio of buildings with different consumption load profiles, PV orientations, system sizes and often include a model of the electricity grid (Strbac et al., 2010, Csetvei, Østergaard and Nyeng, 2011, Baetens et al., 2012, Nykamp et al., 2012). As load profiles differ for each end-user, the surplus electricity produced by a decentralized unit can be consumed by another end-user (IEA, 2014). To maximize the utility's benefits, end-users consumption load profiles can be shaped through active demand response based on a global optimization for the set of connected end-users, regardless of local self-consumption. In the decentralized approach, most studies have focused on the maximization of load matching indicators at the scale of a single building (Vanhoudt, 2012 and Dar et al., 2014). Widén, Wäckelgård and Lund (2009) proposed three options to improve load matching: PV array orientation, optimal load management and additional electrical storage. The two last options were identified as the most effective.

The implementation of demand response programs raises the question of the economic viability for end-users. Indeed, financial benefits are seen as a driving force for residential building owners to invest in new technologies (IEA, 2014). In current net metering programs, for which the resale price is equal to the retail price, the global optimization of the centralized approach does not harm the economic returns of the end-users as long as their surplus production is not curtailed. However, the cost savings for the utility entailed by a large penetration rate of decentralized production is often lower than the cost of compensating this surplus production, and the market model for PV panels is moving towards less attractive surplus resale tariffs (European Commission, 2015). In this context, the optimum electrical load management for the end-user may differ in the centralized and decentralized approaches as net metering programs evolve. In the decentralized approach, to attain grid parity under less attractive economic conditions, the objective for the end-user is no longer to maximize the surplus electricity delivered to the grid, but to maximize its self-consumption (Mondol, Yohanis and Norton, 2009 and Castillo-Cagigal et al., 2011). Kamyar and Peet (2015) carried out a global analysis including utility and customer welfare to determine optimal electricity rates in the presence of demand response programs. Simulations showed that a reduction of electricity bills by up to 20% could be achieved with passive thermal storage and optimal thermostat programming. This entails the need for appropriate load control and right sizing of the PV panels. Zhang and Augenbroe (2014) presented a method to determine optimal PV sizing for a residential U.S. house under different demand response programs and for different locations in the U.S. The method is based on the determination of the maximum net present value based on the influence on curtailing losses of different net metering programs.

The method proposed in the present work is a general methodology for assessing opportunities associated with optimal load management in response to different utility incentives for residential buildings that employ renewable energy sources and energy storage. In light of the above literature survey, the chosen approach is a decentralized optimization to maximize the consumer's benefit through an appropriate control of existing electrical systems, as an incentive to continue promoting the integration of renewable sources in response to changing net metering programs. Net metering allows customers with decentralized electricity production units to supply their excess local electricity production to the electricity grid. A general optimal control solution is proposed to assess the potential of load matching with decentralized production and to study the effects of different buy-back prices on customer economics. The method is illustrated with a case-study of a typical American house equipped with PV panels, an air-to-air heat pump, a water heater and an electrical storage for different buy-back prices. The potential for load matching is characterized in terms of percentage of the electricity production consumed on-site and the proportion of the demand covered by decentralized electricity generation (Baetens et al., 2012 and Van Roy et al., 2013). Guidelines for optimal control of the electrical load and for right-sizing of PV panels are proposed. The price signals used can either be reflective of centralized optimization results maximizing the electricity grid utility's benefits, or can be an image of the congestion level in the distribution grid (as in Csetvei, Østergaard and Nyeng, 2011). It is assumed that the price signal is established in a fair way by the electricity grid utility. Action on the grid (e.g. grid reinforcement) is not considered in the optimization process. The objective is to reduce the burden on the electricity grid while ensuring grid parity for residential prosumers.

The primary uniqueness of this study resides in the general optimal problem formulation to assess the influence of net metering programs on load matching potential. The proposed formulation is very flexible and can be applied to any decentralized power unit and storage system. Moreover, the focus is on the influence of feed in prices rather than forward price signals as in most of the aforementioned studies. The study presents a complimentary approach to the work of Zhang and Augenbroe (2014), for which load shifting and storage were not considered for optimal sizing of the PV system.

The paper is organized as follows. Section 2 presents the billing mechanisms for decentralized renewable production in the U.S. Section 3 details the proposed methodology, including optimal problem statement and system modelling. In Section 4, the methodology is applied to a case study in Indianapolis, IN, with PV panels and different storage systems. Guidelines for right sizing of the systems are proposed. Finally Section 5 concludes the paper.

2. Billing mechanisms

To promote the integration of renewable energy sources, agreements exist between utilities and consumers with grid-connected PV systems. Such consumers are allowed to deliver surplus electricity generated on-site to the local distribution grid following two different existing billing mechanisms. The first mechanism, referred to as net metering, only requires one meter that counts the net power flow to or from the grid. The second option, less widespread in the U.S., meters separately the instantaneous electricity consumption and production. In this case, the electricity is sold back to the utilities at a resale tariff that can differ from the retail tariff.

In the U.S., net metering policies vary according to the states: so far, the excess power generation supplied to the grid is either "bought" at retail or at wholesale price tariffs (U.S.

EIA, 2012). Currently, the retail tariff is applied in most states with net metering programs. From a customer's standpoint, this implies the same economic benefit whether the electricity produced by the PV system is instantaneously consumed on-site or delivered to the grid. There is therefore no incentive to shift the electricity consumption in time to match the local production. With the increase in the number of prosumers, electricity grid congestion and PV curtailment become more frequent, which restricts the amount of distributed power supplied to the grid and tends to modify the economics of surplus electricity sale to the grid.

In this work, a different net metering program is proposed that would promote better load matching between production and consumption. The net electricity flow, i.e. the instantaneous difference between the power consumed and produced on site is determined. If positive, the billing tariff is the retail tariff, π_{ret}. If negative, the excess production is bought back at a buy-back tariff, π_{bb}. One can therefore define the buy-back ratio as

$$\alpha = \frac{\pi_{bb}}{\pi_{ret}} \tag{1}$$

In the following section, the retail tariff chosen as the reference is a flat tariff. The definition easily extends to time-of-use tariffs.

3. Methodology

3.1 Optimal load management formulation

In this section, the general optimal load management problem is specified. The discrete state space representation of the system is summarized by

$$\boldsymbol{x}_{t+1} = f(\boldsymbol{x}_t, \boldsymbol{u}_t, \boldsymbol{w}_t) \tag{2}$$

where $\boldsymbol{x}$ is the state space variable vector, $\boldsymbol{u}$ is the vector of decision variables, i.e. the modular electric power and $\boldsymbol{w}$ is a vector of disturbances.

The total electricity consumption of the consumer at time t, P_t^{cons}, is composed of modular components, $u_{i,t}$, i.e., the consumption of systems that can be adjusted by the optimal load management scheme, and the exogenous consumption, Γ_t, i.e. the share of the electricity consumption that cannot be controlled through load management,

$$P_t^{cons} = \sum_i u_{i,t} + \Gamma_t \tag{3}$$

The net power flow is the difference between the consumption, including storage, and the local electricity production, P_t^{prod}, including storage discharge and decentralized power unit production,

$$P_t^{net} = P_t^{cons} - P_t^{prod} \tag{4}$$

The objective is to minimize the electricity cost for the end-user for a given net metering buy-back ratio, α, which can be expressed as

$$\min \sum_{t=1}^{H} (\max(P_t^{net}, 0) + \min(P_t^{net}, 0)\ \alpha)\ dt \tag{5}$$

with respect to the decision variables and subject to

$$\boldsymbol{x}_t^{min} \leq \boldsymbol{x}_t \leq \boldsymbol{x}_t^{max} \qquad \forall t \in H \tag{5.1}$$

$$\boldsymbol{u}_t^{min} \leq \boldsymbol{u}_t \leq \boldsymbol{u}_t^{max} \qquad \forall t \in H \tag{5.2}$$

$$u_{i,t} + u_{j,t} \leq \max(u_{i,t}, u_{j,t}) \qquad \forall t \in H, i \neq j \tag{5.3}$$

where Equation (5.2) specifies the upper and lower limits for power modulation of the modular components and Equation (5.3) ensures that two related decision variables are not activated simultaneously, as further explained in Section 3.3.

Perfect predictions of the electricity generation by decentralized units and use profiles are assumed (Section 3.2.3) in this paper for the purpose of evaluating the load management opportunities. Based on the known future inputs, the optimizer determines an optimal control response that minimizes the objective function of Equation (5) over the prediction horizon *H* and then applies the control inputs over a defined control horizon *M*, with *M* less than *H*. The prediction horizon is then shifted forward in time to the end of the control horizon, following a so-called "receding horizon" control scheme. The condition *M* less than *H* replaces the use of terminal constraints on the states and allows for an anticipation of the decentralized electricity production.

3.2 Modeling

3.2.1 Case study

The optimal problem presented in Section 3.1 was applied to a typical 4-bedroom single-story ranch-type American house built in the 1990's. Building characteristics have been detailed by Holloway (2013). The building structure consists of a 2-by-4 insulated wood frame on a concrete ground floor. The heated volume is 408m³. The building is equipped with a reversible single speed air-to-air heat pump for space conditioning and an electric water heater for domestic hot water which constitute the flexible thermostatically-controlled loads. High efficiency photovoltaic panels are installed on the roof. An additional electrical storage can be added optionally as flexible load.

3.2.2 Thermal models

A detailed dynamic model of the house is available in TRNSYS (Holloway 2013). The model is detailed regarding the building envelope, but not the equipment (heat pump), as the available data are performance curves from the manufacturer. For the purpose of this work, the heating and cooling demands of the building are determined using a grey-box model trained with yearly simulation results from the detailed TRNSYS model. The grey-box model provides an accurate representation of the thermal response of the house at significantly reduced computational requirements. Root mean square error in free-floating zone temperature prediction was below 0.25°C over a year. Yearly error on total cooling and heating needs is 2.3%. The structure of the model is illustrated in

Figure 1.

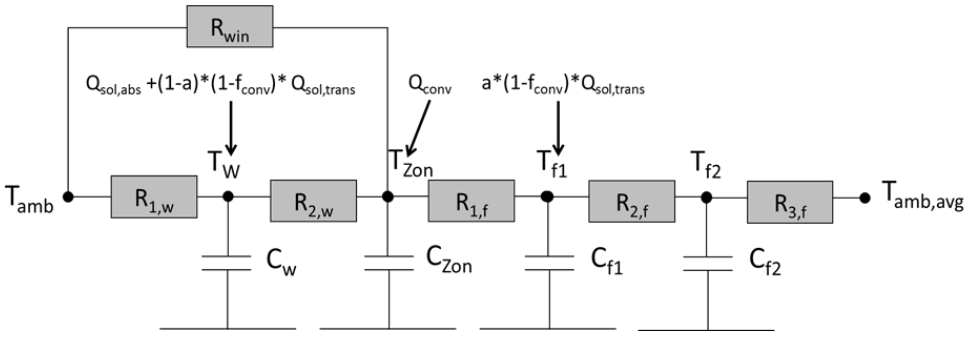

Figure 1: Grey-box model structure

The ground temperature is set to the average annual ambient temperature, $T_{amb,avg}$. The convective thermal power, $Q_{conv,}$ is the sum of the heating (or cooling) power, the internal heat gains due to lighting and occupants, and the convective share of solar gains. No solar protection and no night ventilation in the summer is considered when performing thermal simulation.

The reversible single speed air-to-air heat pump is modelled according to the ASHRAE toolkit model (Brandemuehl, Gabel and Andresen, 1993) in which capacity and coefficient of performance (COP), symbolized by Y in the following equations, are defined as functions of their values at rated conditions (AHRI, 2008) and correction coefficients, f_{Y_T} and f_{Y_m}, taking into account the dependency on the indoor air temperature and humidity, outdoor air temperature, and mass flow rates. Equations in cooling mode are given here below.

$$Y = Y_{rat}\, f_{Y_T}\, f_{Y\,m} \tag{6}$$

with

$$f_{Y_T} = a0 + a1\, T_{amb} + a2\, T_{amb}^2 + a3\, T_{Zon,wb} + a4\, T_{Zon,wb}^2 + a5\, T_{Zon,wb}\, T_{amb} \tag{6.1}$$

$$f_{Y_m} = b1 + b2\, \dot{m}/\dot{m}_{rat} \tag{6.2}$$

In heating mode, the zone wet bulb temperature is replaced by the dry bulb temperature in equations (6.1) and (6.2). All the coefficients for both COP and capacity were derived from performance maps for commercially available heat pumps (Holloway, 2013).

The dependency of the unit performance in cooling mode on the indoor wet bulb temperature has two impacts. First, it introduces a nonlinearity in the system, since the wet bulb temperature is a nonlinear non convex function of the dry bulb temperature and relative humidity. This is further developed in Section 3.3. Secondly, it requires the addition of a moisture model to the building thermal model. A lumped moisture capacitance model is adopted, assuming constant dry air mass in the room, and ten times the air mass capacitance (Rudd, 2013). The continuity equation for water is expressed by the following mass balance

$$m_a \frac{dw_{in}}{dt} = \dot{m}_{a,inf} w_{amb} + \dot{m}_{w,occ} - \dot{m}_{w,cond} - \dot{m}_{a,inf} w_{Zon} \tag{7}$$

where the infiltration and exfiltration rates are assumed to be equal ($\dot{m}_{a,inf}$), $\dot{m}_{w,occ}$ is the amount of water released by the occupants and $\dot{m}_{w,cond}$ is the mass flow rate of water condensing in the cooling coil and given by

$$\dot{m}_{w,cond} = \frac{\dot{Q}_l}{h_{fg}} \tag{8}$$

where h_{fg} is the enthalpy of vaporization.

The latent heat transfer rate, $\dot{Q}_l$, depends on the sensible heat ratio (SHR) of the cooling unit. Two different methods are compared: constant SHR and the by-pass model proposed by Brandemuehl (1993). In the second method, the SHR is defined as a function of the by-pass factor, f_{bp}, as follows

$$SHR = \frac{\dot{Q}_s}{\dot{Q}_s + \dot{Q}_l} = \frac{h(T = T_{in}, w = w_{out}) - h_{out}}{h_{in} - h_{out}} \tag{9}$$

where T_{in} is the temperature of the air at the inlet of the cooling coil, w_{out} is the humidity ratio of the air exiting the coil and

$$h_{out} = \left(1 - f_{bp}\right) h_{adp} + f_{bp}\, h_{in} \tag{9.1}$$

The dependency of the SHR on indoor humidity ratio also introduces a nonlinearity and is further developed in Section 3.3.

Domestic hot water production is provided by an electric water heater equipped with two thermostats and two heating elements located in the upper third and in the lower two-thirds of the tank. Both heating elements cannot be switched on simultaneously, and priority is given to the upper element. Hot water is drawn from the top of the tank and cold water is supplied at the bottom. The water in each part of the tank is assumed to be homogeneously mixed.

3.2.2 Electrical storage model

In addition to the systems traditionally installed in residential buildings, such as electrically-driven heating systems and domestic hot water production systems, an electrical storage can be added. The electricity that flows between the battery and the decentralized power production unit or the electricity grid is modelled by a round-trip efficiency composed of the input efficiency, η_i, which depends on the supply source (AC/DC), the internal battery efficiency, η_{bat}, and the output efficiency, η_o, which corresponds to efficiency of the inverter. Performance degradation with increased number of cycles is not modelled.

The battery state of charge (SOC) is given by

$$SOC_t = SOC_{t-1} + P_t^{supply}\, \eta_i\, \Delta t - \frac{P_t^{discharge}}{\eta_o}\, \Delta t - L_{bat} \tag{10}$$

where the battery losses, L_{bat}, are given by

$$L_{bat} = \frac{P_t^{discharge}}{\eta_o}\left(\frac{1}{\eta_{bat}} - 1\right) \Delta t \tag{10.1}$$

and the internal battery efficiency is assumed constant.

3.2.3 Load profiles

The total building energy demand includes the building space heating (SH) and cooling (AC) loads, the domestic hot water needs and the electricity consumption of appliances and lighting. Water draw-off events as well as appliances and lighting use are modelled by predefined load profiles.

Realistically, it is not likely for the controller to have an exact prediction of the DHW, appliances and lighting events, since they directly relate to unpredictable occupants' behavior. However, typical average load profiles are available and are used for the prediction of the optimal response.

In the "Building America House Simulation Protocols", Wilson et al. (2014) provide a set of data including consumption and typical daily use profiles for an average American dwelling. Profiles for a four-bedroom/two-bathroom dwelling are illustrated in Figure 2. The DHW consumption includes hot water for baths, showers and sinks as well as a dishwasher and a clothes washer. The hot water daily consumption is 265 liters for weekdays and 290 liters on weekends at a supply temperature of about 52°C. For lighting, a seasonal effect is taken into account. The annual electricity consumption for appliances and lighting is 6936 kWh.

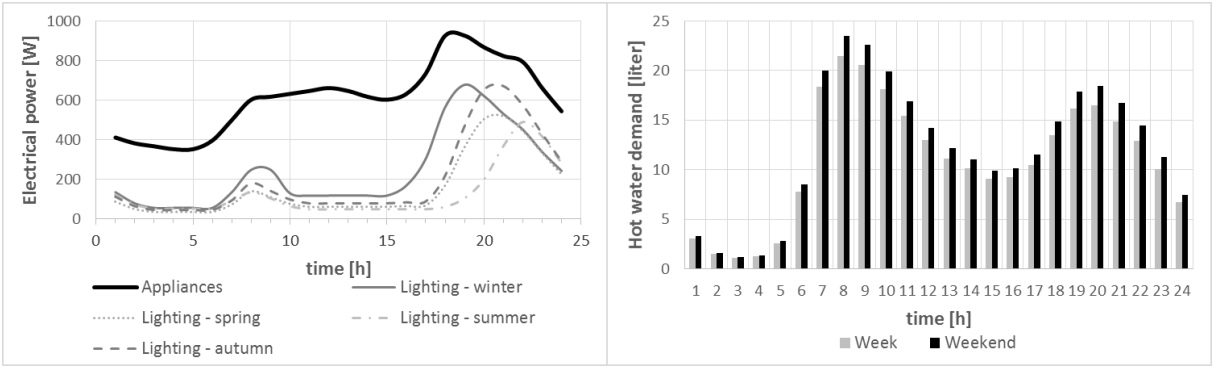

Figure 2: Average daily load profiles: (a) Appliances and lighting – (b) DHW

3.3 State space formulation and linearization

The water heater, battery and grey-box building models allow a straightforward state-space formulation of the governing differential equations as follows

$$\boldsymbol{x}_{t+1} = \boldsymbol{A}\boldsymbol{x}_t + \boldsymbol{B}\boldsymbol{u}_t + \boldsymbol{E}\boldsymbol{w}_t \tag{11}$$

where $\boldsymbol{x}$ is the state space variable vector composed of the zone, wall, first and second floor node temperatures, top and bottom water tank node temperatures, indoor humidity ratio, and battery state of charge,

$$\boldsymbol{x}_t^T = [T_{Zon}, T_W, T_{f1}, T_{f2}, T_{tank_{tp}}, T_{tank_{bt}}, w_{Zon}, SOC] \tag{11.1}$$

$\boldsymbol{u}$ is the vector of decision variables, namely the sensible cooling or heating rate provided by the heat pump to the house ($\dot{Q}_s$), the electric power supplied to the top and bottom parts of the water heater ($P_{WH,tp}$ and $P_{WH,bt}$), the latent thermal cooling rate in the case of cooling ($\dot{Q}_l$), and the battery charging or discharging rate (P_{bat})

$$\boldsymbol{u}_t^T = [\dot{Q}_s, P_{WH,tp}, P_{WH,bt}, \dot{Q}_l, P_{bat}] \tag{11.2}$$

Sign conventions are such that $\dot{Q}_s$ is defined as positive in heating mode and negative in cooling mode, and P_{bat} is taken positive when the battery is charging and negative when discharging.

$\boldsymbol{w}$ is the vector of disturbances, i.e., the outdoor air temperature and humidity ratio, the occupants, lighting and solar gains, the mains water temperature and the rate of hot water used by occupants.

The power consumption expressed in Equation (3) is composed of the power consumed by the heat pump unit, the auxiliary heater, the water heater, the electrical storage and the exogenous consumption corresponding to the consumption of appliances and lighting. Simulations are performed assuming perfect prediction of the electricity consumption profiles of the house.

Constraints (5.1) to (5.3) translate as follows:

- The building zone temperature should remain within a predefined dead band

$$T_{sp,low} \leq T_{Zon} \leq T_{sp,high} \tag{12}$$

  A night set-back strategy is chosen. Over the heating season, $T_{sp,low}$ is set to 18°C during the night and 20°C during the day, while $T_{sp,high}$ is set to 22°C. For the cooling season, the low set point limit is set to 20°C, whereas the high set point limit is set to 24°C during the night and 22°C during the day.

- The water tank temperature in the upper and lower parts should remain within an imposed dead band:

$$T_{sp,low,DHW} \leq T_{tank,bt}, T_{tank,tp} \leq T_{sp,high,DHW} \quad (13)$$

  with $T_{sp,low,DHW}$ and $T_{sp,high,DHW}$ set respectively to 35°C and 50°C in the bottom part and 50°C and 60°C in the top part of the tank.
- The heat delivered to/retrieved from the house should not exceed the full load capacity of the heat pump and auxiliary heater combined in heating mode or of the air-conditioning unit in cooling mode.
- The power supplied to the water tank should remain below the maximum value of each heating element.
- Both hot water tank heaters cannot work simultaneously, which introduces Boolean variables in the optimization problem (Equation (5.3)) and turns the optimization problem into a mixed-integer problem.
- The battery state of charge should remain within a predefined dead-band to avoid deterioration

$$SOC_{min} \leq SOC \leq SOC_{max} \quad (14)$$

  with SOC_{min} and SOC_{max} set respectively to 15% and 95% of the battery capacity.
- The charging and discharging rates of the electrical storage are limited by maximum values specified by the manufacturer.

Feedback control of the HVAC systems is carried out following an "energy rate approach", which considers that the system is allowed to cycle freely to meet the energy requirement for a given simulation time step. Performance degradation due to cycling is taken into account following the method from ASHRAE Standard 116 (1983) and is expressed as a function of the fraction of simulation time step during which the unit is working. The energy rate approach was chosen in order to avoid the use of small time steps that would be needed to explicitly model the dynamic response associated with feedback control.

In the case where no detailed humidity model is included, and constant SHR is assumed, formulation (11) is linear. However, when taking into account the dependency of SHR and unit performance on the indoor humidity ratio, w_{in}, the model becomes nonlinear. Although more difficult to handle, efficient solvers are available to solve nonlinear problems. However, few computationally efficient solvers exist to solve mixed-integer nonlinear problems (MINLP). One solution would require the linearization of all thermodynamics properties of moist air, which is very time-consuming but would be required for real-time application of the proposed method. Since the purpose of this study is to analyse yearly results and parameters of influence, another solution is proposed to linearize the problem. The method consists in considering the error of the indoor humidity estimation as an unpredictable disturbance. The method supposes that the disturbance term is white noise and small (Ljung, 1987) and that the trajectory of the disturbance-free system corresponds to an input sequence w_{in}^* of the indoor humidity ratio, to which corresponds a state trajectory x^*. The linearized form of the system is then

$$\Delta \boldsymbol{x}(k+1) = \boldsymbol{F}\Delta \boldsymbol{x}(k) + \boldsymbol{G}\Delta \boldsymbol{u}(k) + \bar{v}(k) \quad (15)$$

where

$$\Delta \boldsymbol{x} = \boldsymbol{x} - \boldsymbol{x}^* \tag{15.1}$$

$$\Delta \boldsymbol{u} = \boldsymbol{u} - \boldsymbol{u}^* \tag{15.2}$$

and $\bar{v}(k)$ is a white noise disturbance.

In the proposed method, w_{in}^* is obtained based on the estimation of a potential sensible cooling demand. The potential sensible cooling demand, $\dot{Q}_s^*$, is a fraction of the full load sensible capacity. This fraction is assumed to be the ratio of the indoor/outdoor temperature difference over the same difference in rated conditions.

$$\dot{Q}_s^* = \min(\dot{Q}_{s,fl} \frac{T_{amb} - T_{sp}}{T_{amb,c}^{rat} - T_{sp}}, \dot{Q}_{s,fl}) \tag{16}$$

where $\dot{Q}_{s,fl}$ is the sensible cooling capacity at full load, T_{sp} is the room temperature set point, T_{amb} is the ambient temperature and $T_{amb,c}^{rat}$ is the ambient temperature at rated conditions. As a consequence, an approximation of w_{in}, w_{in}^*, is obtained from Equation (7) with a condensing water flow rate given by

$$\dot{m}_{w,cond}^* = \frac{\dot{Q}_{l,fl}}{h_{fg}} \frac{T_{amb} - T_{sp}}{T_{amb,c}^{rat} - T_{sp}} \tag{17}$$

The variable w_{in}^* is initialized to the real value of w_{in} after each control horizon of 12 hours.

Table 1: Mean prediction error for indoor humidity ratio, full load cooling capacity and full load sensible capacity with 1) constant humidity ratio and SHR, 2) indoor humidity modelled by Equations (16)-(17) and constant SHR, 3) indoor humidity modelled by Equations (16)-(17) and SHR from by-pass model.

	Prediction error		
Method	$\boldsymbol{w_{in}}$	$\boldsymbol{\dot{Q}_{tot,fl}}$	$\boldsymbol{\dot{Q}_{s,fl}}$
$w_{in}^* = 0.009424$ kg/kg$_{\text{dry air}}$ and constant $SHR = 0.6$	24.1%	6.7%	13.9%
w_{in} approximated by w_{in}^* and $SHR = 0.6$	14.0%	3.9%	24.3%
w_{in} approximated by w_{in}^* and by-pass model	8.9%	2.5%	5.6%

Three modelling assumptions are investigated to approximate w_{in}. The first method consists of imposing constant humidity ratio and SHR. The second option considers the indoor humidity model proposed in Equations (16) and (17) with constant SHR, and the last method adds the determination of the SHR with the by-pass model. The three methods are compared to a reference scenario based on a conventional tracking of a prescribed indoor set point. This scenario is simulated over four months during the cooling season to obtain a reference profile for w_{in}. The same prescribed control strategy is used to simulate the three modeling approaches. Prediction errors for indoor humidity ratio, full load cooling capacity and full load sensible cooling capacity are summarized in Table 1. Since the optimal load management for space conditioning is based on indoor temperature control, the accurate prediction of the available sensible capacity is of major importance, as it appears as a lower limit in Constraint (5.2). The third method significantly improves the model accuracy in predicting the maximum sensible capacity and is used in the following study.

3.4 Solver

The resulting minimization problem is a convex mixed integer linear programming problem (MILP) solved with the open-source MATLAB compatible toolbox YALMIP (Löfberg 2004) coupled to the CPLEX solver (IBM 2013).Simulations are performed with a one-hour time step, a prediction horizon of 24 hours and a control horizon of 12 hours for a year of simulation.

3.5 Impact indicators

The following grid-impact indicators, first introduced by Baetens et al. (2012), are used to quantify the improvement in load matching brought by the proposed optimal load management scheme.

The supply cover factor, γ_S, represents the percentage of local electricity production consumed on-site

$$\gamma_S = \frac{\sum \min(P^{cons,net}, P^{PV})}{\sum P^{PV}} \tag{18}$$

where $P^{cons,net}$ represents the net power consumed including net power exchange with the electrical storage (charging and discharging).

The demand cover factor, γ_D, represents the percentage of electricity consumption covered by on-site generation

$$\gamma_D = \frac{\sum \min(P^{cons,net}, P^{PV})}{\sum P^{cons,net}} \tag{19}$$

Results are also analyzed in terms of overconsumption due to load shifting, and CO2 emissions.

3.6 System right-sizing

The pay-back time of the system, PB, is defined by Equation (20), and is a function of the net investment costs, C, including tax credit incentives, the retail electricity price, π_{ret}, the interest rate, r, the annual energy consumption, E_{cons}, and the percentage of annual cost savings, S.

$$PB = \frac{C}{\sum_{i=1}^{PB}(S(\alpha, P_{PV}).E_{cons}.\pi_{ret}(1+r)^i)} \tag{20}$$

For the system to be profitable, it should be sized so that the pay-back time does not exceed the expected system lifetime (L), i.e.

$$PB \leq L \tag{21}$$

For a given installed PV capacity, buy-back ratios less than unity tend to decrease the cost savings for the end-user. This increases the pay-back time of the system and reduces the maximum area that can be installed. The optimal control strategy investigated in this paper helps mitigate this pay-back time increase, which, for a given buy-back ratio, allows for the installation of larger systems, compared to a conventional control.

To propose guidelines for right-sizing of PV systems, the optimal control strategy is simulated for a set of buy-back ratios, installed PV capacities and storage. The optimal results are then interpolated to determine the largest system size that satisfies Equation (21), for each buy-back ratio.

4. Results and discussion

4.1 Influence of net metering programs

As mentioned in Section 3.2.1, the building investigated is a typical 4-bedroom single-story ranch-type American house built in the 1990's (Figure 3). The envelope insulation levels meet standard efficiency code (ICC 2003) for the climate zone associated with the city of Indianapolis in the Midwest (zone number 5, ICC 2009). Overall air-to-air heat transfer coefficients (U values) for walls, roof and windows and a breakdown of the annual electricity consumption are given in Figure 3. High efficiency photovoltaic panels are installed on the west slope of the roof of the house. The choice of orientation can be justified by the interest of a mid-afternoon peak PV production in the case of high peak electricity consumption in the evening and in the absence of additional electrical storage. For the following results, a total surface of PV panels of 30m², equivalent to 50% annual load coverage is considered. Table 2 summarizes the characteristics of each system. The weather data used in the simulations are hourly values of solar irradiation and meteorological elements for Indianapolis, IN for a one-year period based on the National Solar Radiation Data Base updated for years 1991 to 2005.

U values [W/m²K]	
External walls	0.41
Roof	0.17
Windows	1.96

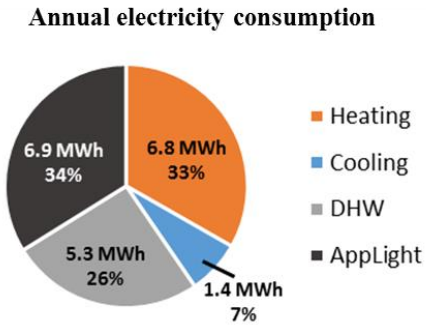

Figure 3: Ranch house (reproduced from Holloway, 2013) – Building envelope characteristics and breakdown of annual electricity consumption.

Table 2: Systems characteristics summary for ranch-type house.

	Systems characteristics – Ranch house	
Heat pump	Heating capacity / COP	11.7 kW / 3.7
	(rated conditions for heating)	*(47°F/70°F)*
	Cooling capacity / COP	11.3 kW / 3.9
	(rated conditions for cooling)	*(95°F/80°F)*
	Back up electric heater	5 kW
Water heater	Volume	0.189 m³
	Lower / upper element heating power	4.5 kW / 4.5 kW
PV panel	Annual load coverage (surface)	10 – 100% (6 – 60 m²)
	Efficiency	21.5% (PV manufacturer, 2014)

Five net-metering tariffs are investigated, out of which four are flat tariffs with buy-back ratios set respectively to 1, 0.75, 0.25 and 0.01. A fifth tariff following a predefined daily profile is used where the buy-back ratio is equal to one during peak demand hours (7 to 9 am and 6 to 8 pm) and to 0.1 during off-peak hours. Results are presented in terms of annual demand and supply cover factors (Section 3.5), total annual electricity consumption, and cost savings for the consumer compared to the costs without PV collectors. Results for the different cases are summarized in Table 3. It should be noted that these results constitute an upper limit on the load matching potential, and that in practice, buy-back tariffs of less than 1 might only be applied during time-periods of grid congestion.

Table 3: Supply/demand cover factors, total electricity demand and total cost for five net metering tariffs. Cost savings are compared to a case without PV collectors.

	Optimal control				***No optimization***			***Comparison***
α	γ_D [ ]	γ_S [ ]	P_{cons} $[MWh/y]$	Cost saving [%]	γ_D [ ]	γ_S [ ]	Cost saving [%]	Cost saving increase
1	0.27	0.59	18.80	50.3%	0.28	0.64	43.9%	6.4%
0.75	0.30	0.65	18.82	46.3%	0.28	0.64	40.0%	6.4%
0.25	0.33	0.70	19.02	39.4%	0.28	0.64	32.1%	7.3%
profile	0.32	0.69	19.19	39.6%	0.28	0.64	31.3%	8.3%
0.01	0.34	0.75	19.41	36.4%	0.28	0.64	28.3%	8.1%

For a control strategy without optimal load management, which consists in the tracking of a prescribed temperature set point, the demand and supply cover factors have no dependence on buy-back ratio. Conversely, for optimal load management that decreases surplus PV production, both demand and supply cover factors increase with decreasing buy-back ratio. When the electricity surplus sale price is reduced from 100% to 75% of the retail price, demand and supply cover factors increase by about 3% and 6%, respectively, with optimal control. A less significant improvement (3% and 5%) is observed when reducing the tariff from 75% to 25%. The total cost savings for the consumer diminishes by 4% and 10.9% when the PV production buy-back price is reduced respectively from 100% to 75% and from 100% to 25%. The results in terms of cover factors obtained with the variable tariff for peak and off-peak periods (predefined daily profile) are very similar to those obtained for a flat buy-back price of 25% of the retail price. For the present case study, with limited storage capacity, the values for the demand and supply cover factors approach 0.34 and 0.75, respectively, for a buy-back tariff approaching zero. A monthly analysis of the cover factors is summarized in Table 4. As expected, the demand cover factors are higher in the summer, whereas the supply cover factors are higher in the winter.

Despite the increase in on-site consumption of local electricity production with lower net-metering tariffs, the total electricity consumption cost for the consumer seems to increase (Table 3). However, the cost savings should not be compared between the different tariffs. For the same tariff enforced by the electricity supplier, optimizing the consumer's load profile to match PV production brings up to about 8.1% additional cost savings compared to results without optimization.

Table 4: Supply and demand cover factors – monthly analysis

	γ_D			γ_S		
α	*Mean*	*Min (month)*	*Max (month)*	*Mean*	*Min (month)*	*Max (month)*
1	0.27	0.11 (12)	0.57 (7)	0.59	0.47 (4)	0.89 (1)
0.75	0.30	0.12 (12)	0.62 (7)	0.65	0.53 (5)	0.98 (1)
0.25	0.33	0.13 (12)	0.66 (7)	0.70	0.58 (5)	0.99 (1)
profile	0.32	0.13 (12)	0.63 (7)	0.69	0.57 (5)	0.99 (1)
0.01	0.34	0.13 (12)	0.68 (7)	0.75	0.63 (5)	0.99 (1)

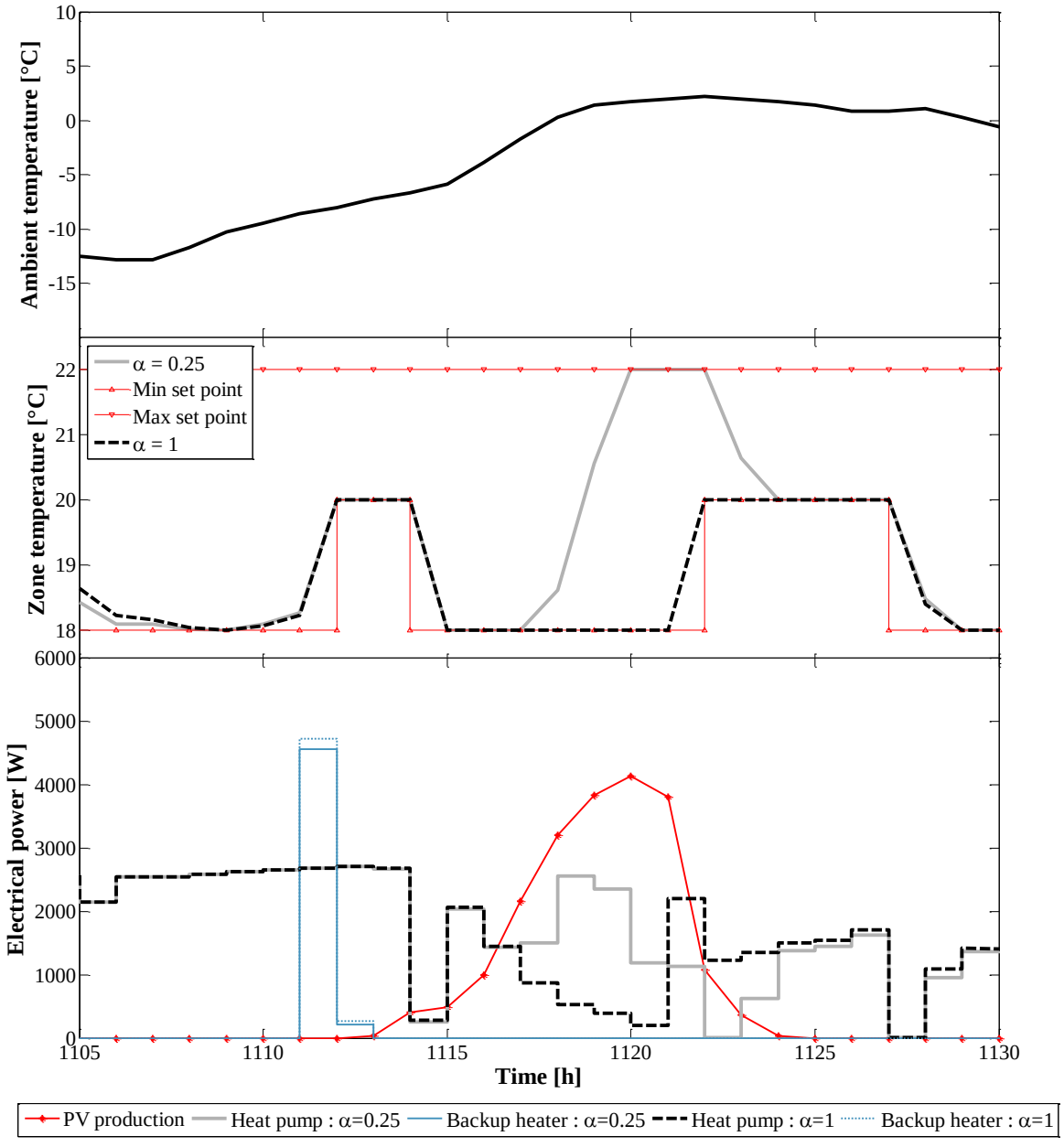

Figure 4: Bottom – Electrical power consumption for space heating for α=1 and α=0.25 and PV production for February 15th. Top – Corresponding zone and ambient temperatures.

Figure 4 and Figure 5 compare example optimal responses obtained for two buy-back tariffs: 100% and 25% of the retail price. As can be observed in Figure 4, for lower net-metering tariffs, the optimal control tends to shift the heat pump electrical demand to periods of time with simultaneous PV production. The building zone is preheated in order to lower the electricity consumption during periods of time with the absence of sun. For the example shown in Figure 4, preheating the indoor air allows the heat pump to remain off for the next hour, and to work for shorter time periods the following hours. An analogous trend is observed in Figure 5 for the electric water heater. Preheating the water typically allows for up to a three-hour slowdown of the system.

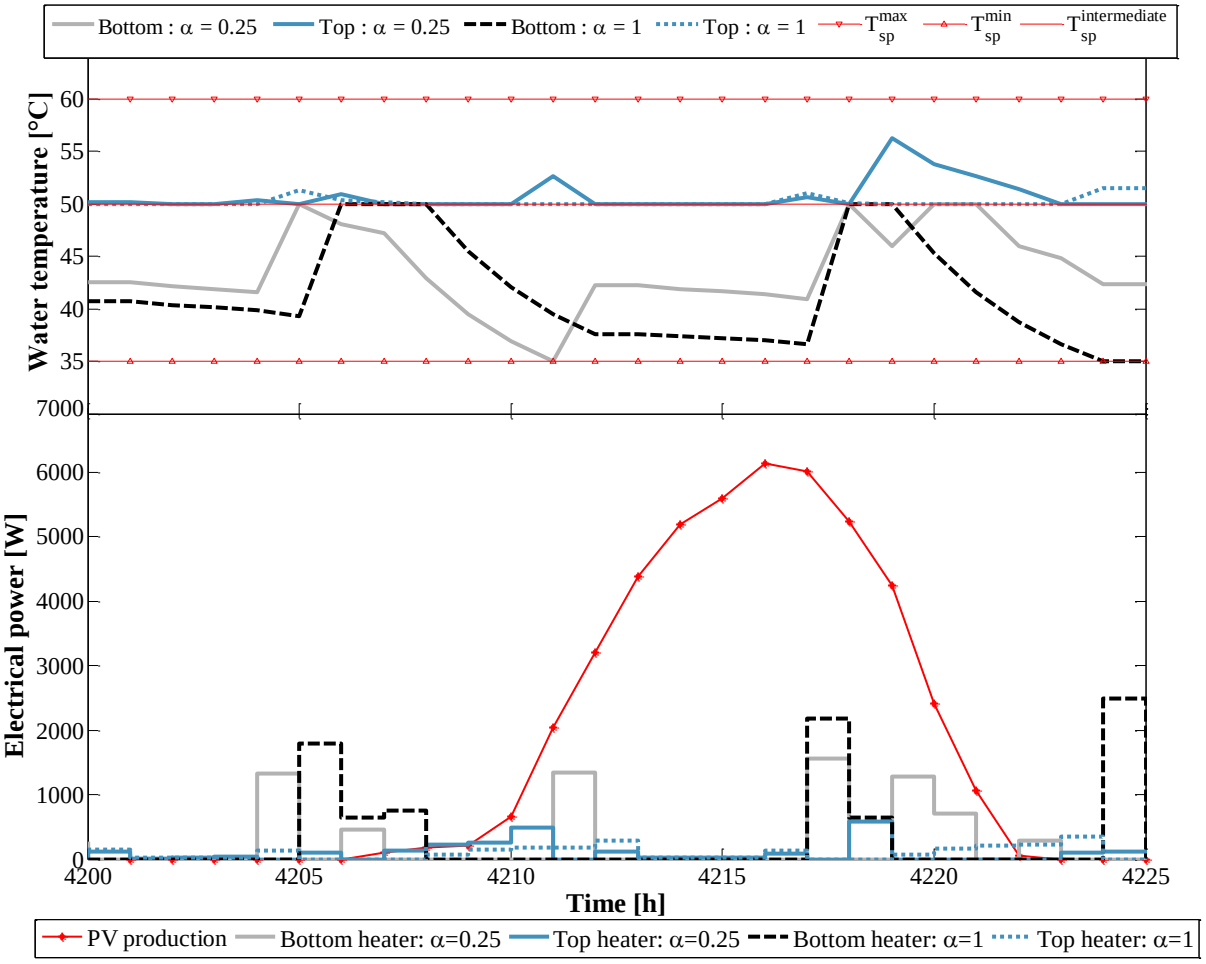

Figure 5: Bottom – Electrical power consumption for DHW for α =1 and α =0.25 and PV production for June 24th. Top – Corresponding water tank lower and upper thermostat temperatures.

The amount of load shifted by using the DHW heaters and the heat pump varies with the buy-back ratio and the period of the year. Figure 6 shows the monthly additional load shifted by each system towards periods with PV production, for buy-back ratios of 0.75 and 0.01 compared to a buy-back ratio equal to unity. For a buy-back ratio of 0.75, the incentive to shift the load is not very strong and the amount of load shifted is relatively homogeneous throughout the year. During the summer, most of the load shifted is ensured by the water heaters. Indeed, shifting the heat pump demand to periods of the day with warmer ambient temperatures increases the heat pump consumption, which in turn may be less profitable than

selling the excess PV production at a reduced resale price. In contrast, for a buy-back ratio of 0.01, contrariwise, the monthly evolution of the load shifting potential is directly correlated to the amount of PV production. The amount of load shifted using the building structure as thermal storage is about two times larger than with the water heater. It should be noted that the values obtained are strongly dependent on temperature dead bands set as constraints, and would differ for a building with higher thermal inertia.

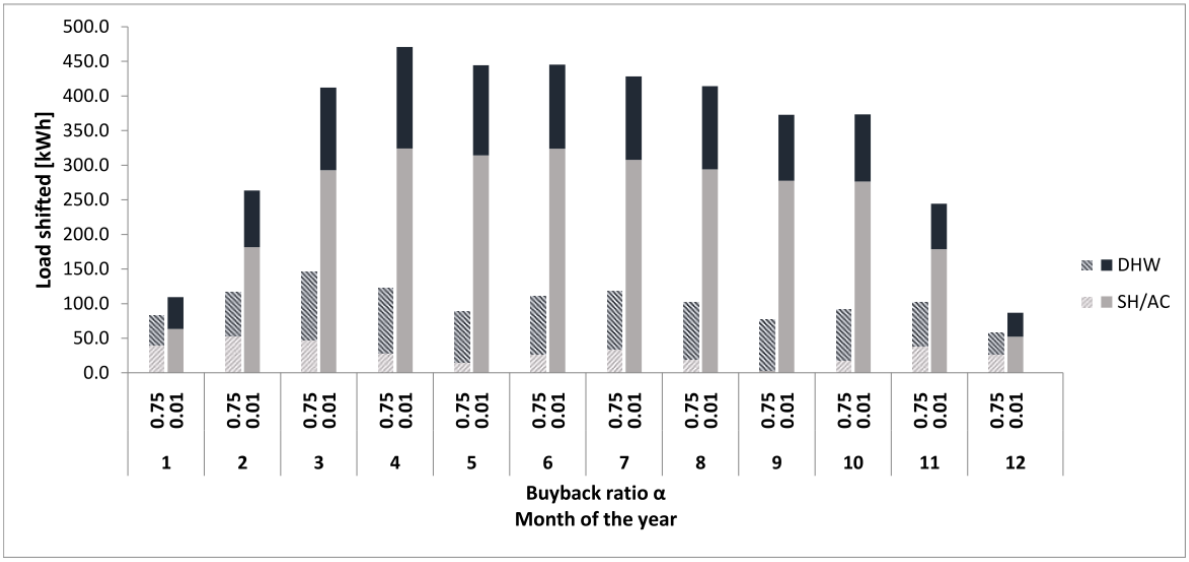

Figure 6: Thermal load shifted to match PV production per month for DHW and space heating or air-conditioning (SH/AC)

Finally, the optimal total electricity demand profile obtained with the time-varying net-metering pricing is illustrated in Figure 7. Load matching is enforced during off-peak hours, typically in the afternoon when the PV production is maximum. This also tends to shift part of the morning and night consumption peaks to off-peak periods, but not as significantly as for constant tariffs. Indeed, since surplus electricity production can be sold at a higher price during these periods, it remains interesting for the consumer to deliver electricity back to the grid. Therefore, flat tariffs seem more suitable as an incentive for load matching.

Load shifting to increase load matching also leads to an increase in the total annual electricity consumption of up to 3.3% (Table 3) compared to a buy-back ratio of unity. Figure 8 identifies the sources of overconsumption. During the heating season, as the buy-back ratio decreases, the slightly higher set points achieved tend to increase the ambient heat losses and can slightly deteriorate the COP of the heat pump. In cooling mode, the heat transfer through the building envelope increases due to lower set points. The average COP tends to improve for a buy-back ratio of 0.75, as the unit works closer to full load which reduces performance degradation due to cycling losses. For lower buy-back ratios however, this effect is counterbalanced by the performance degradation due to greater operation of the unit during time periods with high ambient temperatures. The relative share of heat losses from the water tank tend to diminish with decreasing buy-back ratios, but the absolute value of energy wasted increases. One could argue that overconsumption could counter-balance the benefits retrieved from using on-site renewable electricity production in terms of CO2 emissions. This is discussed in Section 4.4.

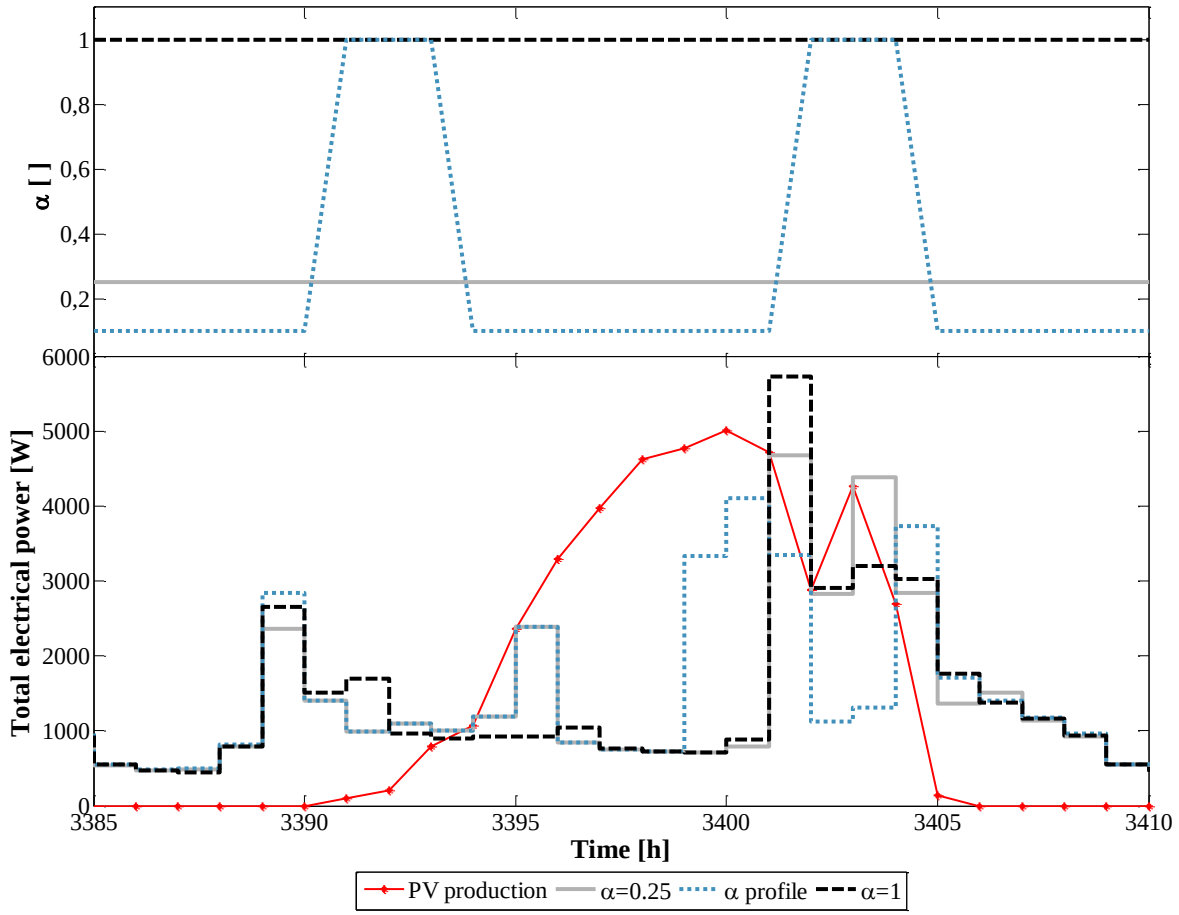

Figure 7: Comparison of total electricity consumption and PV production for α following a daily profile (1 during peak hours and 0.1 during off-peak hours), α=0.25 and α=1.

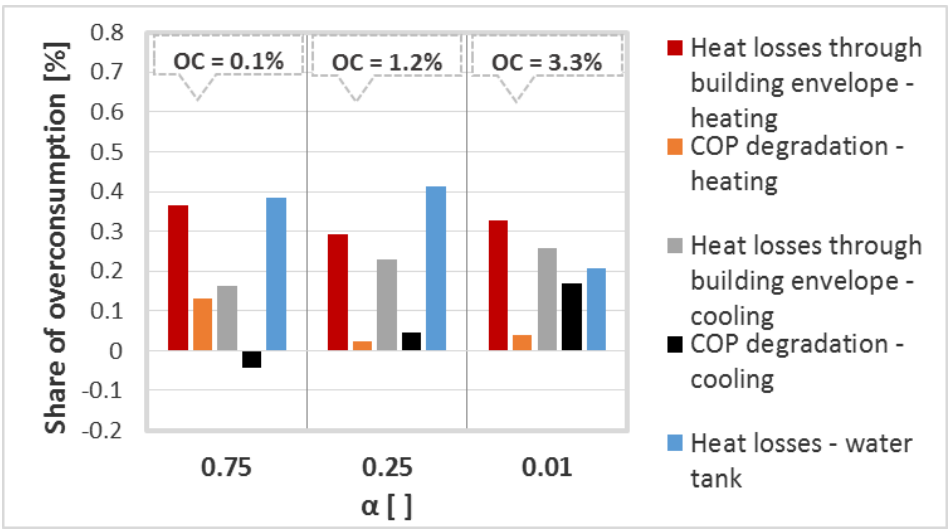

Figure 8: Sources of overconsumption compared to buy-back ratio of unity.

4.2 Influence of thermal storage

The building considered in the above sections is a typical light wooden structure for residential construction in the U.S. Similarly, the volume of the water tank is set to the average value for a 4-bedroom house, i.e. 189 liters, which is less than the average daily

DHW use (Section 3.2.3). The storage capacity for load shifting is therefore limited, and it is worth investigating the load matching potential attained with additional thermal storage. Two options are considered here. In the first case, the thermal inertia of the building is increased by replacing the light wooden structure by heavy concrete walls. The overall U-value remains unchanged.

Figure 9a shows the additional percentage of load shifted for space conditioning as a function of the buy-back ratio. The additional percentage of load shifted is greater with the heavy structure, but the increase becomes less significant as the buy-back ratio decreases. The heavy structure also allows for slightly more efficient load shifting with less overconsumption and increased cost savings (Table 5 – left). The second option consists in increasing the size of the DHW tank. Other standard DHW tank sizes available on the market are 300 liters and 450 liters. When decreasing the buy-back ratio from one to zero, up to 3.1% additional DHW electricity consumption can be shifted to match PV production, compared to results with the baseline tank volume, as shown in Figure 9b. However, additional overconsumption of up to 2.8% is observed. The additional cost savings, without taking into account the extra investment for a larger water heater, reach up to 5.2% (Table 5 – right).

Table 5: Cost savings increase – Left: heavy vs light structures – Right: DHW tank volume. Cost savings increase are determined compared to a case without optimal control.

	Cost saving increase	
α	*Light*	*Heavy*
1	6.4%	7.2%
0.75	6.4%	7.3%
0.25	7.3%	8.9%
0.01	8.1%	10.1%

	Cost saving increase	
Volume [m³]	$\alpha = 1$	$\alpha = 0.01$
0.189	6.4%	8.1%
0.300	6.4%	11.4%
0.450	6.3%	13.3%

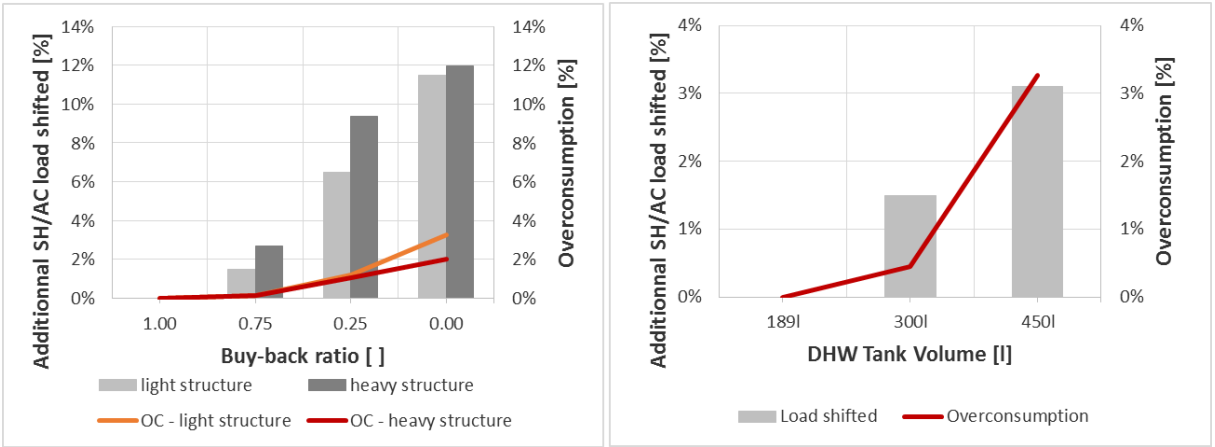

Figure 9: (a) Additional SH/AC load shifted and overconsumption (OC) with light and heavy building structures (left). (b) Additional DHW load shifted and overconsumption (OC) with increasing water heater tank volume and a buy-back ratio of 0.01, compared to a tank volume of 189 liters and a buy-back ratio equal to unity (right).

Other options exist, such as replacing the ducted heating system by a radiant floor heating with additional water storage tank. This requires significant changes and is better suited for new construction rather than as a retrofit option. They are worth investigating in future work.

4.3 Additional electrical storage

An additional electricity storage system was added to the systems used in section 4.2 and additional simulations were performed. The characteristics are provided in Table 6. It was found that with a flat electricity tariff, buy-back ratio of one, and round trip efficiencies less than 100%, then optimal control leads to no utilization of the battery regardless of the battery capacity and PV system sizing. In other words, it makes no sense to utilize a battery if the utilities will buy back electricity at the same rate they sell it, except for ensuring security of supply in the case of power outage. However, as the buy-back ratio decreases from one to zero, the use of the battery helps increase cost savings and load cover factors, as shown in Table 7 for fifty percent load coverage by west-oriented PVs and a battery size of 7kWh. The maximum cost savings at a buy-back ratio 0.01 are only about 5%, resulting from increased demand and supply cover factors. The use of south-oriented PV panels led to an additional cost savings of 4% compared to west-orientated ones. However, overconsumption resulting from load shifting went up by 17% in that case.

Table 6: Battery characteristics (manufacturer data, 2015).

	Systems characteristics – Ranch house	
Battery	Capacity	7 kWh – 10.5 kWh – 14 kWh
	Maximum charge/discharge rate	3.3 kW
	DC/DC roundtrip efficieny	0.92
	Battery cost	429$/kWh
	Inverter and installation cost	1500$

Table 7: Results for west-oriented PVs with 50% load coverage: comparison between thermal storage only and an additional battery of 7kWh.

	Thermal storage			***Thermal + electrical storages***			***Comparison***
α	γ_D [ ]	γ_S [ ]	Cost saving [%]	γ_D [ ]	γ_S [ ]	Cost saving [%]	Cost saving increase
1	0.59	0.27	50.3%	0.59	0.27	50.3%	0.0%
0.75	0.65	0.30	46.3%	0.80	0.37	47.1%	0.8%
0.25	0.70	0.33	39.4%	0.83	0.38	43.0%	3.6%
0.01	0.75	0.34	36.4%	0.87	0.39	41.3%	4.9%

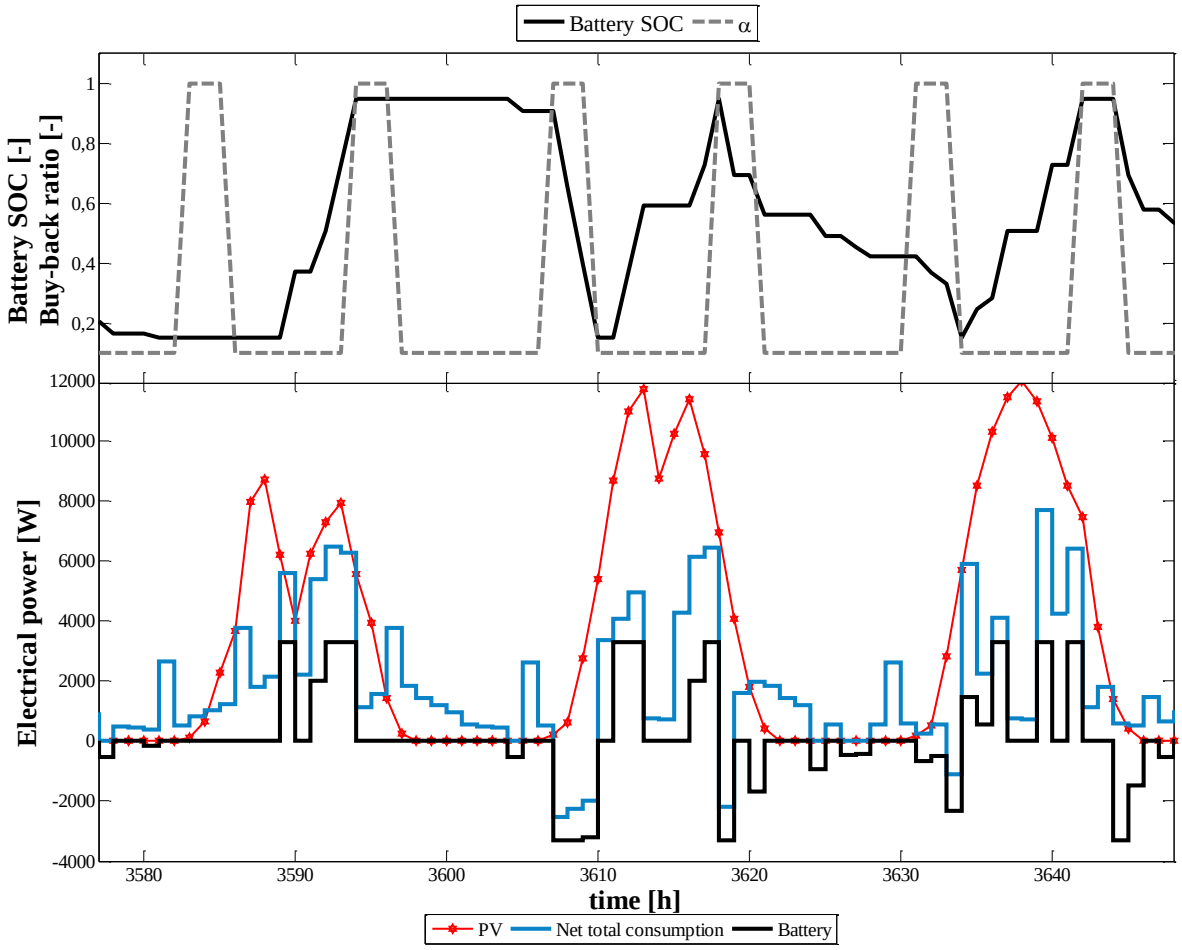

Figure 10: Top: Battery state of charge and buy-back ratio profile for 3 days in the spring with south-oriented PVs, an annual PV load coverage of 100%, and a battery capacity of 14kWh. Bottom: Corresponding PV production, net electricity consumption and battery power.

With a flat retail tariff and a constant buy-back ratio, the optimal control stores the excess PV production in the battery, but never supplies it back to the electricity grid. To consider the possibility of resale of the electricity stored in the battery to the grid, the buy-back ratio profile presented in section 4.1 was used and is illustrated in Figure 10 (top). This profile encourages the sale of excess PV production or the resale of electricity stored in the battery to the grid during time periods with high buy-back ratios. Electrical power management is illustrated in Figure 10 (bottom) for an area of south-oriented PV-panels ensuring 100% annual load coverage and a battery capacity of 14kWh for three days of the spring season. The optimal control stores surplus electricity produced by PVs when the buy-back ratio is equal to 0.1 and releases it either to the grid when the buy-back ratio is equal to unity or directly supplies the house when there is a lack of PV production. In this particular case, 14% of the annual energy released by the battery is directly sold back to the grid.

4.4 Guidelines for system right-sizing

This section illustrates how cover factors and consumer pay-back times change with the size of the PV installation for different buy-back ratios and different storages. In the US, the average installation cost of PV panels was 3.27 $ per watt peak in 2015 (NREL 2015). No significant scale benefits can be observed for an installed power in the range of 5kW$_p$ to 10

kW_p. A federal tax credit incentive provided 30% reduction of the cost for residential PV systems (IREC 2012). The electricity retail tariff for residential consumers in Indiana was 0.11 $/kWh. For the scenario with an electrical battery, investment costs were composed of 1500$ for the inverter and the installation of the system, and of 429$ per kWh of installed capacity. For the scenario with larger DHW tanks, the additional cost is about 350$ per hundred liters.

The case-study system of Section 4.1, with a DHW tank of 189L, is chosen as reference for this section. For this system, two control strategies are simulated: a strategy based on a conventional tracking of a prescribed indoor set point, referred to as rule-based control (RBC), and the optimal control strategy proposed in this paper, referred to as OPC. Three areas of PV panels are considered: 50%, 100% and 200% annual load coverage. For each of them, a comparison is performed between the reference case and the case-study system with either a water heater of 300L or three different battery sizes.

The impact of varying PV system size and storage type on the demand cover factor is presented in Figure 11 for a buy-back ratio of 0.01. Compared to the RBC reference, the increase in demand cover factor reaches up to 33%. Figure 12 illustrates the pay-back time reduction brought by the OPC formulation, compared to the RBC reference, for a buy-back ratio of 0.01. Reductions of 11% to 25% are observed depending on the load coverage and storage. With 50% PV load coverage, thermal storages lead to larger reduction in pay-back time, as the excess PV production to store in the battery is limited. For 100% PV load coverage, increasing the water heater volume from 189L to 300L decreases the pay-back time by a value close to the one obtained when using a 7kWh battery. For larger PV coverage, pay-back time reductions increase significantly with the capacity of the electrical storage.

The use of electrical storage brings significant cost savings for the end-user. However, if the lifetime of the system is limited to 30 years for PVs and 10 years for an average domestic battery, none of the configurations with a battery investigated here are actually economical in the case of a buy-back ratio of zero. With the adopted assumptions on investment cost, pay-back times range from 15.4 years for the reference system to 37.3 years for the largest PV areas and battery storage. Conclusions may differ for time-varying buy-back ratios and retail tariffs.

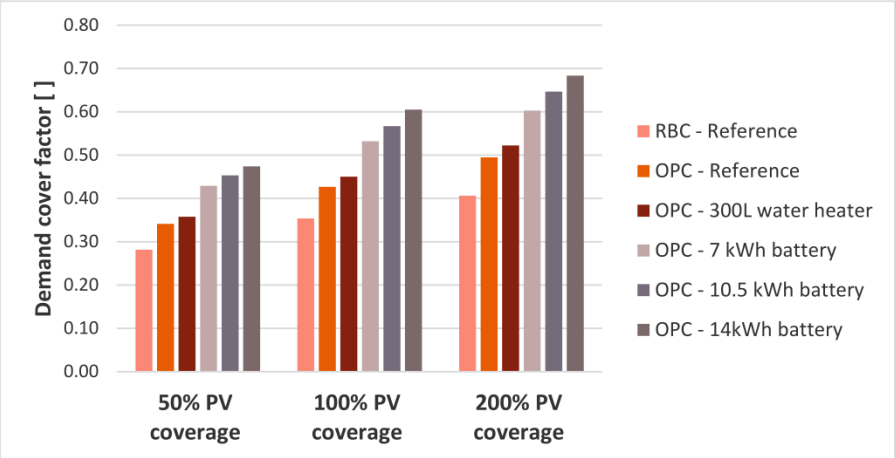

Figure 11: Evolution of the demand cover factor between the reference case of section 4.1 with rule-based control (RBC) and optimal control (OPC) with the default systems, a water heater of 300L and three battery sizes for PV annual load coverages of 50%, 100% and 200% and a buy-back ratio of 0.01.

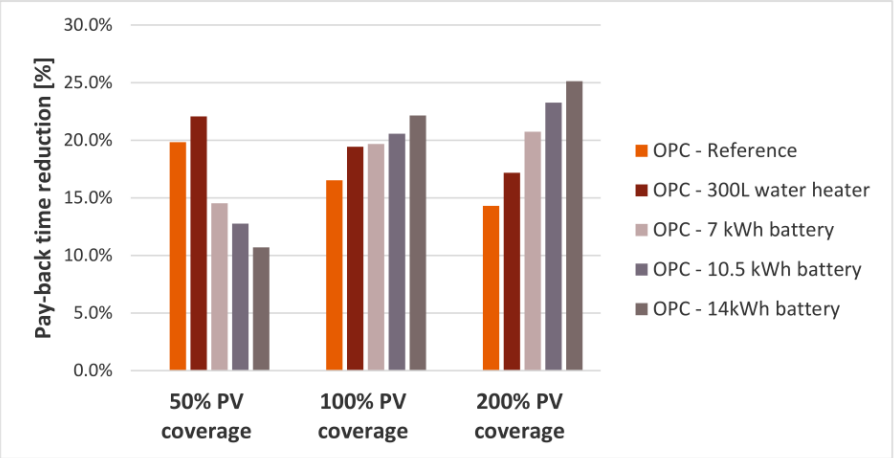

Figure 12: Evolution of the pay-back time reduction with optimal control (OPC) of the default systems, a water heater of 300L and three battery sizes for PV annual load coverages of 50%, 100% and 200% and a buy-back ratio of 0.01 compared to the reference case.

Figure 13 shows the reduction in CO2 emissions for each case based on monthly average hourly data for the electricity production mix of RFC West subregion (OpenEI, 2011). These values were generated based on demand profiles of year 2008 and constitute the most comprehensive database available. With thermal storage only, the reductions reach 11% to 21%, whereas with additional electricity storage, the reductions increase to 22% to 46%.

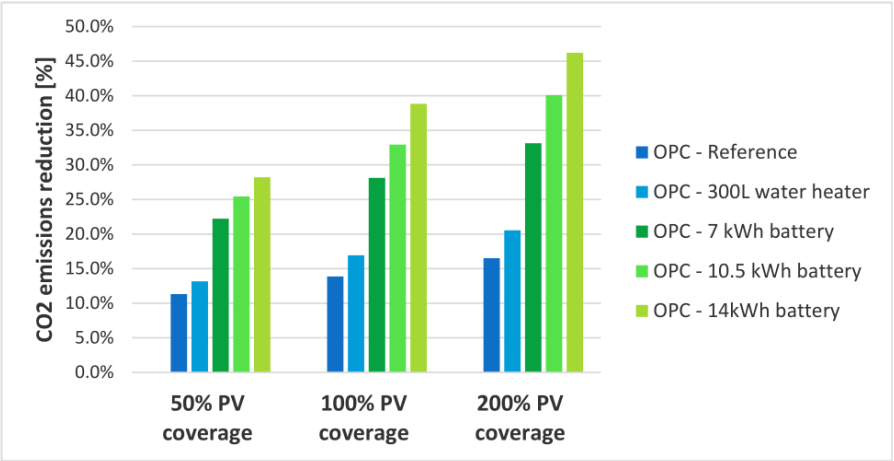

Figure 13: CO2 emissions reduction with optimal control (OPC) of the default systems, a water heater of 300L and three battery sizes for PV annual load coverages of 50%, 100% and 200% and a buy-back ratio of 0.01 compared to the reference case.

As thermal storage offered by the building envelope and the water heater are naturally available in any house, a deeper analysis of the right sizing of PV panels with thermal storage only is proposed here after. The total surface of PV panels was varied between 10% to 100% annual load coverage. As expected, for approximately the same total electricity consumption, the demand cover factor increases with the surface area of PV panels. However, the same tariff incentive promotes load shifting to different extents depending on the PV area. The largest load coverage by PV for a given buy-back ratio can be obtained from Equation (21). For this case study, Figure 14a compares the consumer's pay-back time for optimized and non-optimized load management as a function of the buy-back ratio for different PV areas. The pay-back time increases significantly with decreasing buy-back ratios, and especially for

larger PV areas. For buy-back ratios decreasing from 1 to 0.25, the pay-back time for non-optimized load control increases by 14%, 30% and 62%, respectively, for 30%, 50% and 100% annual load coverage. Optimizing load profiles to match on-site PV production reduces this increase by 7% to 10%.

Thus, for net-metering programs with buy-back ratios less than one and no other economic incentives, installing larger PV areas without increasing on-site storage capacity to promote load matching may become unprofitable. Given a life expectancy of about 30 years for PV panels, optimum sizing of PV panels, expressed in terms of percentage of the annual electricity consumption covered, can be derived for each buy-back ratio. Results are illustrated in Figure 14b. For a buy-back ratio of 1, there is no theoretical limit, and a maximum of PV panels should be installed. For buy-back ratios less than 0.3, an optimum value arises. The maximum coverage goes down to 62% for non-optimized load profiles and 75% for optimized ones as the buy-back ratio approaches zero. These conclusions are closely linked to net metering programs implemented in this study. The electricity supplier could promote other incentives in parallel, such as payoffs to prosumers who optimize on-site electricity consumption.

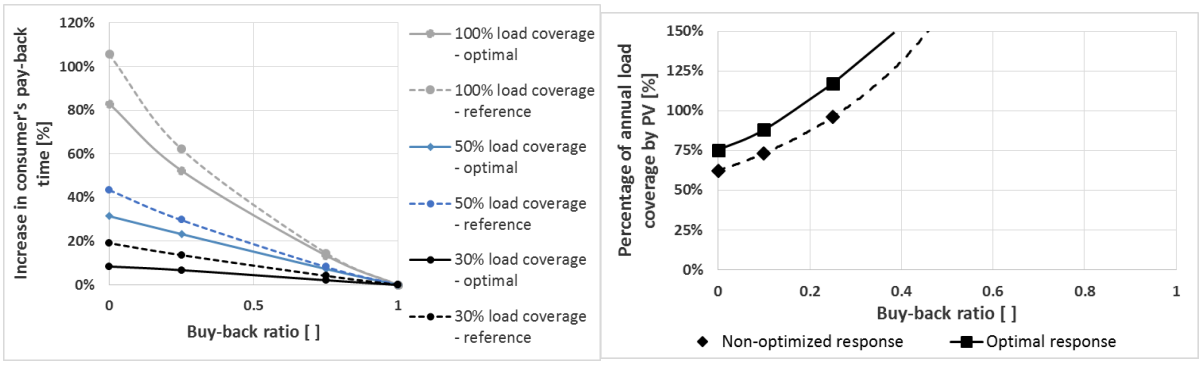

Figure 14: (a) Increase in consumer's pay-back time as a function of the buy-back ratio for three different load coverages (30%, 50%, 100%) (top) – (b) Optimal load coverage by PV vs buy-back ratio (bottom).

Several parameters are likely to influence the above results, such as system investment costs, retail electricity tariffs and electricity production mix. For example, significant differences exist between the different zones of the US. Average retail tariffs range from 0.069 to 0.34 $/kWh (IEA, 2013). The impact of the buy-back ratio on the system pay-back time decreases with the increase in retail tariff and new optimal load coverage can be determined. Average CO_2 emissions in the U.S. vary between 369 to 789 kg/MWh of produced electricity (OpenEI 2011). Depending on the electricity production mix, overconsumption entailed by load shifting may counterbalance reductions in emissions by increased onsite consumption of renewable energy. Projections regarding PV installation cost reach 1.5$ per watt peak (DOE, 2014) and battery cost of 137$/kWh (CSIRO, 2015) by 2035. Conclusions regarding the economic viability of thermal and electrical storage will be impacted.

6. Conclusions

In this study, a general method for optimal management of decentralized electricity production unit and HVAC system with storage in response to evolving net metering programs is proposed. It is expected that future utility incentive programs will seek to minimize the excess electricity production delivered to the grid by promoting on-site

consumption through the use of different net metering tariffs. The optimal load management methodology was applied to a case study consisting in a typical U.S. house equipped with a reversible heat pump, an electric water heater, a battery and PV panels in the city of Indianapolis.

Results show that imposing a tariff lower than the retail tariff for the excess electricity generated proved to be a good incentive to promote load matching. For the particular case of Indianapolis, the yearly percentage of demand directly covered by on-site generation increased by 3 to 28% depending on the available storage capacity. In terms of potential improvement in load matching, the choice of a flat tariff seems more suitable than a time-varying tariff. In all cases, the increase in load matching is not proportional to the diminution in the tariff for a given installed PV power. Despite the increase in cover factors, the overall electricity cost for the consumer increases with a lower buy-back tariff. However, for the same tariff enforced by the electricity supplier, optimizing the consumer's load profile to match PV production brings between 6.4 and 27.5% additional cost savings. With the current electricity retail tariff and the assumed investment costs for PV systems and battery, the additional cost savings brought by electrical storage are not sufficient for such systems to be economical. Thermal storage is a better economic choice in the short-term. Despite overconsumption due to load shifting of up to 4.2%, CO_2 emissions reductions of 11 to 46% are observed.

The proposed method also allowed the determination of the optimal sizing of the decentralized production system for a given storage capacity and buy-back ratio. Indeed, for larger PV areas, reducing buy-back tariffs has a less significant impact on load matching improvement, and increases dramatically the consumer's pay-back time. For heating-dominated climates, optimal load management with thermal storages allowed for an increase of 13 to 21% in the optimal size of the system.

In future work, the impact of the parameters of influence identified in the study could be further investigated, such as different climate conditions, electricity production mix and retail tariffs. The buy-back tariff could be adjusted to reflect the level of grid congestion or demand management strategies based on a global optimization at the scale of a district. Other financial incentives from the electricity supplier could be investigated, such as complimentary payoffs for prosumers optimizing their load profiles to reduce their impact on the grid. Finally the impact of the occupant's behavior could be introduced as a disturbance through stochastic load profiles for DHW draw-off events and appliances and lighting use.

References

Air-conditioning, Heating and Refrigeration Institute (AHRI), 2008, "Performance Rating of Unitary Air-Conditioning & Air-Source Heat Pump Equipment", No. 210/240-2008, 211 Wilson Boulevard, Suite 500, Arlington, VA 22201, USA.

American Society of Heating, Refrigerating and Air Conditioning Engineers (ASHRAE), 1983, "Standard 116: Methods for Rating Seasonal Efficiency of Unitary Air Conditioners and Heat Pumps", Atlanta, Georgia, USA.

American Society of Heating, Refrigerating and Air Conditioning Engineers (ASHRAE), 2013, "Handbook of Fundamentals", Atlanta, Georgia, USA.

Baetens, R., De Coninck, R., Van Roy, J., Verbruggen, B., Driesen, J., Helsen, L., Saelens, D., 2012, "Assessing electrical bottlenecks at feeder level for residential net zero-energy buildings by integrated system simulation", *Applied Energy*, vol. 96, pp. 74-83. doi: 10.1016/j.apenergy.2011.12.098.

Bollen M., Hassan F., 2011, "Integration of Distributed Generation in the Power System", 1st ed., John Wiley & Sons, IEEE press, Piscataway, NJ, USA.

Brandemuehl, M. J., Gabel, S., & Andresen, I., 1993. "HVAC 2 Toolkit: A Toolkit for Secondary HVAC System Energy Calculations", American Society of Heating, Refrigerating and Air-Conditioning Engineers, Atlanta, Georgia, USA.

Castillo-Cagigal, M., Caamano-Martín, E., Matallanas, E., Masa-Bote, D., Gutiérrez, A., Monasterio-Huelin, F. and Jiménez-Leube, J., 2011, "PV self-consumption optimization with storage and active DSM for the residential sector". *Solar Energy*, vol. 85(9), pp. 2338-2348.

Csetvei, Z., Østergaard, J., Nyeng, P., 2011, "Controlling Price-Responsive Heat Pumps for Overload Elimination in Distribution Systems", In Innovative Smart Grid Technologies (ISGT Europe), pp. 1-8.

CSIRO, 2015, *Future energy storage trends - An assessment of the economic viability, potential uptake and impacts of electrical energy storage on the NEM 2015–2035, Report No. EP155039.*

Dar, U. I., Sartori, I., Georges, L., and Novakovic, V., 2014, "Advanced control of heat pumps for improved flexibility of net-ZEB towards the grid", *Energy and Buildings*, vol. 69, pp. 74-84. doi: 10.1016/j.enbuild.2013.10.019.

De Coninck, R., Baetens R., Saelens, D., Woyte A. and Helsen L., 2014, "Rule-based demand side management of domestic hot water production with heat pumps in zero energy neighborhoods", *Journal of Building Performance Simulation,* Vol. 4(7), pp. 271–288. doi: 10.1080/1940149YYxxxxxxxx.

European Commission, "Best practices on Renewable Energy Self-consumption", COM(2015) 339 final, Brussels, July 2015.

Halvgaard, R., Poulsen, N. K., Madsen, H., & Jorgensen, J. B., 2012, "Economic model predictive control for building climate control in a smart grid", In *Innovative Smart Grid Technologies (ISGT)*, 2012, pp. 1-6. doi: 10.1109/ISGT.2012.6175631.

Holloway, S., 2013, "An annual performance comparison of various heat pumps in residential applications", MS thesis, Purdue University, IN, USA.

IBM ILOG, 2013, CPLEX Optimization Studio.

International Code Council (ICC). 2003, 2009, "International Energy Conservation Code (IECC)".

International Energy Agency (IEA), 2014, "Task 40/Annex 52: Towards Net Zero Energy Solar Buildings Load Match and Grid Interaction in NZEB with high-resolution data", report of Subtask A.

Interstate Renewable Energy Council (IREC), 2012, "Database of State Incentives for Renewables and Efficiency (DSIRE) - Residential Renewable Energy Tax Credit"

Kamgarpour M., Ellen C., Soudjani S. E. Z., Gerwinn S., Mathieu J. L., Müllner N., Abate A., Callaway D. S. Fränzle M., Lygeros J., 2013, "Modeling Options for Demand Side Participation of Thermostatically Controlled Loads", IREP Symposium-Bulk Power System Dynamics and Control - IX, August 25-30, Rethymnon, Greece.

Kamyar, R. and Peet, M. M., 2015, "Optimal Thermostat Programming and Optimal Electricity Rates for Customers with Demand Charges", in *American Control Conference*, July 1–3th 2015, Chicago, Illinois, USA.

Ljung, L., 1987, *Book Title: System identification – theory for the user*, New Jersey: PTR Prentice Hall.

Löfberg J., 2004, "YALMIP: A Toolbox for Modeling and Optimization in MATLAB", In *Proceedings of the CACSD Conference*, Taipei, Taiwan.

Mitchell, J.W. and Braun, E. J., 2013, *B*ook Title: Principles of Heating, Ventilation, and Air Conditioning in Buildings, New Jersey: John Wiley & Sons.

Mondol, J. D., Yohanis, Y.G. and Norton, B., 2009, "Optimising the economic viability of grid-connected photovoltaic systems", *Applied Energy*, vol. 86(7), pp. 985-999.
doi: 10.1016/j.apenergy.2008.10.001

National Renewable Energy Laboratory (NREL), 2007, "National Solar Radiation Database 1991–2005 Update".

National Renewable Energy Laboratory (NREL), 2013, "The Open PV Project", https://openpv.nrel.gov/

Nykamp, S., Molderink, A., Bakker, V., Toersche, H.A., Hurink, J.L. and Smit, G.J.M, 2012, "Integration of Heat Pumps in Distribution Grids: Economic Motivation for Grid Control", 3rd IEEE PES International Conference and Exhibition on Innovative Smart Grid Technologies (ISGT Europe), Berlin, Germany, October 14th-17th.

OpenEI, 2011, "Hourly Energy Emission Factors for Electricity Generation in the United States", [online] http://en.openei.org/datasets/dataset/hourly-energy-emission-factors-for-electricity-generation-in-the-united-states

Reza Miara, M., Günther, D., Leitner, Z. L., & Wapler, J., 2014, "Simulation of an Air-to-Water Heat Pump System to Evaluate the Impact of Demand-Side-Management Measures on Efficiency and Load-Shifting Potential", *Energy Technology*, vol. *2*(1), pp. 90-99. doi: 10.1002/ente.201300087.

Rudd, A., 2013, "Expert Meeting: Recommended Approaches to Humidity Control in High Performance Homes", U.S. Department of Energy (DOE), July 2013.

Sartori I., Napolitano A., Voss K., 2012, "Net zero energy buildings: a consistent definition framework", *Energy and Buildings*, vol. 48, pp. 220-232. doi: 10.1016/j.enbuild.2012.01.032.

Strbac, G. et al., 2010, "Energy Networks Association Benefits of Advanced Smart Metering for Demand Response based Control of Distribution Networks", executive summary, Centre for Transport Studies, Imperial College, London, England.

U.S. Department of Energy (DOE), 2012, *2011 Buildings energy data book,* Energy Efficiency & Renewable Energy.

U.S. Department of Energy (DOE), 2014, *Photovoltaic System Pricing Trends Historical, Recent, and Near-Term Projections,* 2014 Edition

U.S. Energy Information Administration (EIA), 2012, "Policies for compensating behind-the-meter generation vary by State", *Today in Energy*, May 9th, 2012.

U.S. Energy Information Administration (EIA), 2013, "2013 Retail Power Marketers Sales-Residential", [online] http://www.eia.gov/electricity/sales_revenue_price/

Vanhoudt, D. (VITO), 2012, "Lab test results of an active controlled heat pump with thermal energy storage for optimal integration of renewable energy". *International renewable Energy Storage Conference*.

Van Roy J., Salenbien R., Vanhoudt D., Desmedt J. and Driesen J., 2013, "Thermal and Electrical Cover Factors: Definition and Application for Net-Zero Energy Buildings", in *Proceedings of CLIMA 2013 Conference*, Prague, Czech Republic, 16-19 June 2013.

Widén, J., Wäckelgård, E. and Lund, P. D., 2009, "Options for improving the load matching capability of distributed photovoltaics: Methodology and application to high-latitude data", *Solar Energy*, vol. 83, pp. 1953–1966. doi: 10.1016/J.SOLENER.2009.07.007.

Wilson E., Engebrecht Metzger, C., Horowitz S., Hendron R., 2014, "2014 Building America House Simulation Protocols", National Renewable Energy Laboratory, Technical Report NREL/TP-5500-60988.

Zhang, Y. and Augenbroe, G., 2014, "Right-sizing a residential photovoltaic system under the influence of demand response programs and in the presence of system uncertainties", in

Proceedings of Building Simulation Conference, September 10-12th 2014, Atlanta, Gerorgia, USA.

Acknowledgements

F.R.S. - FNRS (Fond de la Recherche Scientifique - FNRS) in Belgium is gratefully acknowledged for the funding of Emeline Georges as a PhD research fellow.

Nomenclature

Symbols		**Subscripts/Superscripts**	
C	thermal capacity, investment cost	a	air
E	energy (Wh or J)	abs	absorbed
f	fraction	adp	apparatus
h	enthalpy	amb	ambient
H	prediction horizon	avg	average
L	system lifetime	bb	buy-back
m	mass	bp	bypass
M	control horizon	bt	bottom
P	electrical power (W)	c	cooling
Q	heat transfer capacity	cond	condensation
R	thermal resistance	cons	consumption
S	savings	conv	convective
T	temperature	ex	exhaust
u	decision variable	f	floor
w	disturbance	fl	full load
x	state variable	in	indoor/inlet
Y	thermal capacity or COP	inf	infiltration
		l	latent
Greek		m	mass flow rate
α	buy-back ratio	net	net
π	electricity price	occ	occupant
Γ	exogenous consumption	out	outlet
		PV	photovoltaic
		rat	rated
		ret	retail
		s	sensible

su	supply
sol	solar
sp	set point
T	temperature
t	time
tp	top
trans	transmitted
w	wall
wb	wet bulb
WH	water heater
win	window
Zon	zone